CHEMISTRY
A EUROPEAN JOURNAL

DOI: 10.1002/chem.200801250

Label-Free Colorimetric Detection of Trace Atrazine in Aqueous Solution by Using Molecularly Imprinted Photonic Polymers

Zhen Wu, Cheng-an Tao, Changxu Lin, Dezhong Shen, and Guangtao Li*[a]

Abstract: Based on the combination of colloidal-crystal templating and a molecular imprinting technique, a sensor platform for efficient detection of atrazine in aqueous solution has been developed. The sensor is characterized by a 3D-ordered interconnected macroporous structure in which numerous nanocavities derived from atrazine imprinting are distributed in the thin wall of the formed inverse polymer opal. Owing to the special hierarchical porous structure, the molecularly imprinted polymer opals (or molecularly imprinted photonic polymer; MIPP) allow rapid and ultrasensitive detection of the target analyte. The interconnected macropores are favorable for the rapid transport of atrazine in polymer films, whereas the inherent high affinity of nanocavites distributed in thin polymer walls allows MIPP to recognize atrazine with high specificity. More importantly, the atrazine recognition events of the created nanocavities can be directly transferred (label-free) into a readable optical signal through a change in Bragg diffraction of the ordered macropores array of MIPP and thereby induce color changes that can be detected by the naked eye. With this novel sensory system, direct, ultrasensitive (as low as 10^{-8} ng mL^{-1}), rapid (less than 30 s) and selective detection of atrazine with a broad concentration range varying from 10^{-16} M to 10^{-6} M in aqueous media is achieved without the use of label techniques and expensive instruments.

Keywords: atrazine · chemosensors · colorimetric detection · molecular imprinting · polymers

Introduction

Owing to the selectivity against broadleaf weeds and annual grasses, atrazine is the one of the most widely used herbicides for combating weeds in corn, sugarcane, and sorghum crops.[1,2] Along with the benefit for modern agriculture, however, the large-scale application of this herbicide resulted in the contamination of drinking water and soil through various pathways into the environment, causing serious health risks even at very low (sub ppb) levels.[3] The United States Environmental Protection Agency (USEPA) has found short-term atrazine exposure above the drinking water maximum contaminant level (MCL) to potentially cause heart, lung, and kidney congestion, low blood pressure, muscle spasms, weight loss, and damage to adrenal glands.[2] Long-time exposure to atrazine concentrations above the drinking water MCL may induce more severe diseases. Therefore, the development of a facile analytical method to efficiently and rapidly monitor or detect atrazine levels is highly desirable.

Currently existing technologies to detect trace atrazine in various samples mainly include gas chromatography (GC), gas chromatography–mass spectrophotometry (GC/MS), high-pressure liquid chromatography (HPLC), liquid-chromatography mass spectrophotometry (LC/MS), and enzyme-linked immunosorbent assay (ELISA).[1–4] Although all of these methods have shown sensitivity and specificity for the detection of atrazine, they are mostly cumbersome, time-consuming, and expensive, and require complicated clean-up procedures or sophisticated technical equipment. As a result, there has been considerable interest in the development of alternative technologies for rapid, sensitive, and inexpensive detection of atrazine,[5–7] with the ideal situation being that detection could be visualized through a pH-like test paper by the naked eye.

Recently, using colloidal-crystal templating to create materials with 3D-ordered interconnected macroporous structure has drawn considerable interest for the development of various chemical and biological sensors.[8–9] Owing to the periodic porous structure, such materials (inverse opals) exhibit fascinating optical properties (Bragg diffraction) and

[a] Z. Wu, C. Tao, C. Lin, Prof. D. Shen, Prof. Dr. G. Li
Key Lab of Organic Optoelectronics & Molecular Engineering
Department of Chemistry, Tsinghua University
Beijing, 100084 (China)
Fax: (+86) 10-6279-2905
E-mail: LGT@mail.tsinghua.edu.cn

bright structural color. Particularly, if these highly ordered macroporous materials are made from responsive polymer hydrogels, they are able to swell or shrink in aqueous solution upon molecular recognition or environmental conditions to change the periodic spacing, leading to a change in optical properties. In this respect, several research groups have introduced molecular recognition elements or stimuli-responsive units into the 3D-ordered skeleton.[8–16] For instance, through the incorporation of a crown ether, boronic acid, or pH-sensitive group, Watanabe and co-workers fabricated inverse opal-based sensors that are highly sensitive to metal ions, ionic strength, pH change, or glucose concentration.[11–14] Interestingly, through rational choice of pore size, they can design the color change at a given detection concentration. Using this approach, Braun and co-workers also developed several remarkable chemo- and biosensors.[15–16] Inspired by these studies, we recently developed a new concept for constructing photonic-based sensors by using the combination of colloidal-crystal templating and molecular imprinting techniques.[17] Molecular imprinting is a well-established and facile technique used to synthesize molecularly imprinted polymers (MIPs) with specific molecular recognition nanocavities.[18–22] Owing to the complementarity in shape and binding sites, the created nanocavities can act as artificial antibodies and exhibit high selectivity towards the imprinted molecules, including a large and diverse set of important organic or bioorganic molecules or metal ions. This combination of both templating techniques (colloidal-crystal templating and molecular imprinting) affords 3D highly ordered and interconnected macroporous arrays with a thin polymer wall in which nanocavities that are complementary to analytes in shape and binding sites are distributed. Such a hierarchical porous structure is especially beneficial in sensor applications that require high specific surface areas, more interaction sites, efficient mass transport, and easier accessibility to the active sites through the interconnected macroporous system, as well as high specificity to analytes of the nanocavities. More importantly, in this molecular system, the molecular recognition events of the created nanocavities will give rise to a readable optical signal through a change in diffraction properties of ordered macroporous arrays that accompanies a visually perceptible color change.

Our preliminary work confirmed the feasibility of our new concept described above and a novel L-dopamine sensor was developed.[17] As an extension of our work and further demonstration that the developed concept is possible for the construction of pH-paper-like molecularly imprinted systems, the biologically significant molecule atrazine was chosen as a target. Furthermore, the feasibility of developing a convenient but efficient approach for label-free colorimetric detection of trace atrazine in aqueous solution based on a molecularly imprinted photonic polymer (MIPP) was investigated.

Results and Discussion

Fabrication of atrazine-imprinted photonic polymers: Atrazine was chosen as the targeted molecule as it is one of the most widely used herbicides. For a comparative study, two 1,3,5-triazines (ametryn and prometryn) that are structurally similar to atrazine as well as one structurally unrelated herbicide (2,4-dichlorophenoxyacetic acid, 2,4-D) were used as reference compounds in this work (Scheme 1).

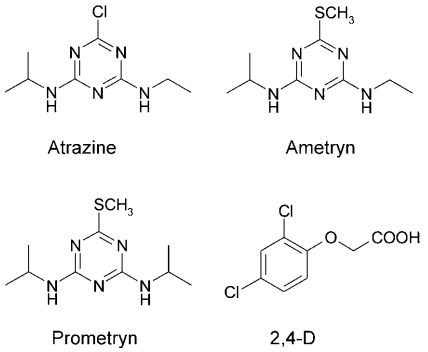

Scheme 1. Chemical structures of the herbicides used.

Scheme 2 displays a three-step approach employed for the construction of atrazine-imprinted photonic polymer hydrogels, including the preparation of a colloidal-crystal template, the polymerization of the pre-ordered complex of atrazine with functional monomers in the interspacers of the colloidal crystal, and the removal of the used templates (colloid particles and atrazine molecules). Silica colloidal-crystal arrays prepared by vertical deposition on glass substrates were used as templates for the formation of 3D highly ordered macroporous structure. The size of monodispersed silica particles can be tuned in the range of 150–400 nm by changing the fabrication conditions. In the present work, monodispersed silica spheres with a diameter of 186 nm were used to form a close-packed face-centered cubic (fcc) photonic crystal film with a thickness of about 2 μm. The atrazine-imprinted polymer hydrogel was prepared by a noncovalent, self-assembly approach. The template molecule (atrazine), functional monomer, and cross-linking agents were first mixed to generate a pre-polymerization cluster that utilizes hydrogen-bond interactions, electrostatic attraction, and associated weak interactions. The mixture was then filled into the void spaces of the colloidal-crystal array by capillary force by using a sandwich structure (see the Experimental Section). Upon polymerization, the structure was frozen in a 3D network of polymers. The removal of silica particles and the embedded atrazine molecules from the imprinted polymer matrix affords 3D highly ordered and interconnected macroporous arrays with specific nanocavities that could specifically interact with the atrazine molecule through noncovalent interactions.

For a successful creation of nanocavities that show excellent specificity, the efficiency of complexation between the

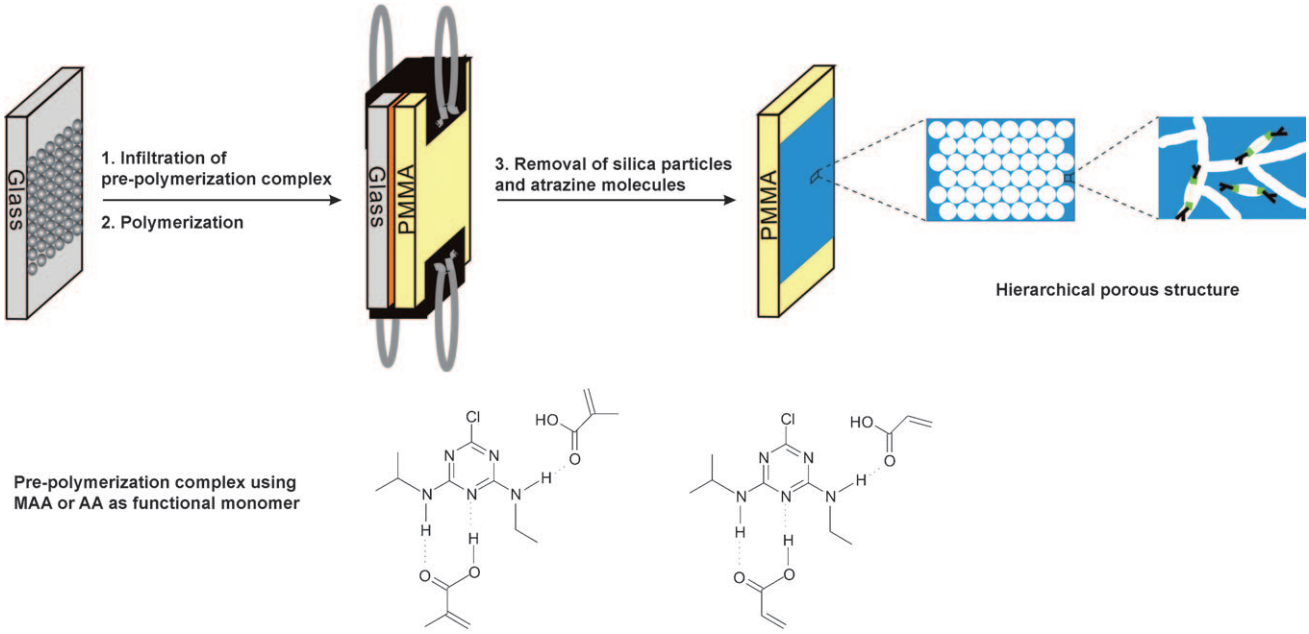

Scheme 2. Schematic illustration of the procedure used for the preparation of the molecularly imprinted photonic polymer (MIPP).

print molecule and the functional monomers is critically important. Therefore, aside from the optimization of the polymerization conditions, extensive studies in the molecular imprinting area have focused on the selection of suitable functional monomers and increasing complexation efficiency.[26–27] In the case of atrazine, several research groups have prepared molecularly imprinted polymers by using methacrylic acid (MAA) as a functional monomer.[27–32] Dual hydrogen bonding is expected to occur between atrazine and MAA as a key interaction necessary for binding-site construction (see Scheme 2), in which a carboxylic group of MAA works as both a hydrogen-bond acceptor and a donor that interacts with a hydrogen atom of the amino group and a nitrogen atom of atrazine body, respectively. Takeuchi and co-workers performed NMR spectroscopic studies and found that the addition of MAA into the atrazine solution resulted in low-field shifts of peaks derived from the ethylamino and the isopropylamino protons of atrazine.[29] This suggests that hydrogen and/or nitrogen atoms of the amino groups of the atrazine are invloved in hydrogen-bond formation. The three remaining nitrogen atoms of the core of the atrazine structure could also be involved in hydrogen bonding as hydrogen acceptors. Based on these studies, we first used MAA as the functional monomer, and its complexation with atrazine molecules was cross-linked with ethylene glycol dimethylacrylate (EGDMA) at a molar ratio of 1:4:1 (atrazine/MAA/EGDMA) to form the nanocavities in the 3D macroporous skeleton. Figure 1 shows the typical SEM images of the used colloidal-crystal template and the resultant atrazine-imprinted photonic polymer hydrogel film with a thickness of about 2 μm.

Sensing properties of the MAA-based MIPP film: Conventional molecular imprinting techniques only afford thousands to millions of highly specific binding pockets or recognition elements that, like their biological receptor counterparts, possess the ability to recognize and bind specific target molecules. As a sensing element, the integration of these recognition elements with an appropriate transduction element is required. In our case, however, owing to the 3D-ordered porous structure, the signal can be generated by the molecularly imprinted polymer hydrogel itself through Bragg diffraction, and the molecular recognition process can be directly transferred into readable optical signals.

The diffraction peak, λ_{max}, for the porous hydrogel is determined by the Bragg equation (1):

$$\lambda_{max} = 1.633(d/m)(D/D_0)(n_a{}^2 - \sin\theta^2)^{1/2} \quad (1)$$

where D is the sphere diameter of the silica colloidal particle, m is the order of Bragg diffraction, (d/d_0) is the degree of swelling of the gel (d and d_0 denote the diameters of the gel in the equilibrium state at a certain condition and in the reference state, respectively), n_a is the average refractive index of the porous gel at a certain condition, and θ is the angle of incidence. According to this equation, if the molecular recognition process could cause the swelling or shrinkage of the prepared hydrogel, the readable optical signal may be detectable.

We examined the sensing response of MAA-based MIPP to atrazine with a series of concentrations of atrazine in 5 mM phosphate buffer solution at pH 7.6. Figure 2 displays the sensing behavior of the photonic polymer hydrogel fabricated by using the pre-polymerization mixture with atrazine/MAA/EGDMA in a 1:4:1 molar ratio. The original hy-

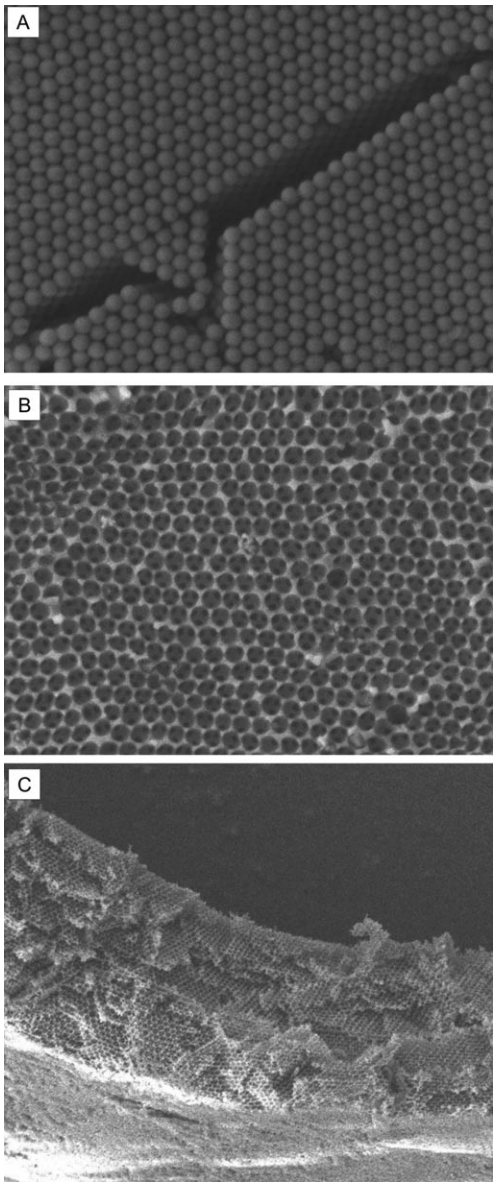

Figure 1. SEM images of the used colloidal-crystal template (A), the formed MIPP film (B), and a cross-section of the MIPP film (C).

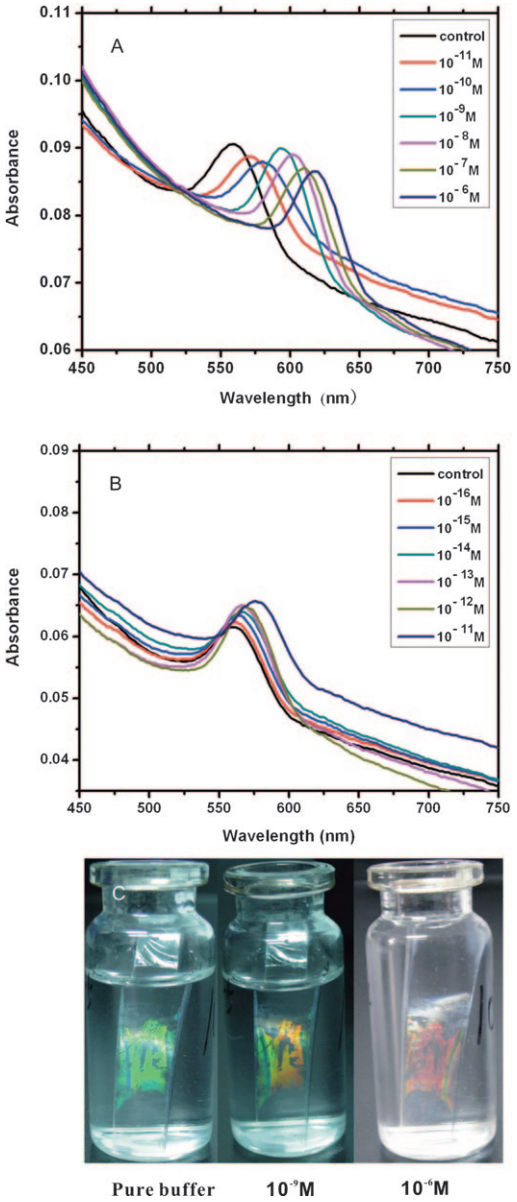

Figure 2. Optical response of MAA-based MIPP to atrazine with a series of concentrations: A) concentration range 10^{-6} to 10^{-11} M; B) concentration range from 10^{-11} to 10^{-16} M; C) color change induced by the rebinding of atrazine at different concentrations.

drogel shows well-defined Bragg diffraction at 558 nm and exhibits good single-color diffraction. It is found that this optical diffraction of MIPP is very sensitive to the rebinding of the atrazine molecule. Upon exposure to 10^{-12} M atrazine in phosphate buffer solution for 2 min, the diffraction peak of MIPP shifts to 572 nm. With the increase in the concentration of atrazine, the peak gradually shifts to the longer-wavelength region (Figure 2A). The peak of the EIPP film soaked in 10^{-6} M atrazine is already redshifted by 60 nm relative to that of the original blank EIPP in phosphate buffer solution. The color changes that accompany the peak shift of the Bragg diffraction also are visually evident. The blank EIPP film in the phosphate buffer solution is a green-yellow color. After the exposure to 10^{-9} M and 10^{-6} M atrazine solution, the EIPP film changed color to orange (594 nm) and red (618 nm), respectively (Figure 2C).

Importantly, we found that the EIPP film is capable of detecting trace amounts of atrazine. Even in lower concentration solutions of atrazine (10^{-12} M–10^{-16} M), a clear redshift of the Bragg diffraction was also detectable and the detection limit of 0.1 fM was reached (Figure 2B), which is seven orders of magnitude lower than that reported for the established methods so far. To demonstrate that the induced diffraction shift is not due to the impurity of the solution, we also performed control experiments by preparing solutions that are identical to those described above, but in the absence of atrazine. The EIPP film was exposed to these sam-

ples one after another for a fixed period. As expected, the diffraction shift was not detected in the absence of atrazine. In this work, the sensing response of MAA-based MIPP to atrazine was also examined in 5 mM phosphate buffer solution at pH 2.5. However, no Bragg diffraction shifts were observed. The possible reason is that the nanocavities resulting from MIP are so small that carboxy groups located nearby could form hydrogen bonds directly by themselves, preventing template molecules from penetrating into the gel network. Recently, the pH sensitivity of MAA-based inverse opal was also investigated.[15]

Encouraged by these promising results, we have also tried different polymerization recipes, including adjusting the molar ratio between atrazine, functional monomer, and cross-linker as well as changing the solvents used. However, the maximum Bragg shift of the resulting MAA-based MIPP films is only 60 nm and does not cover the whole visible-light wavelength range. As a result, we focused our attention on finding another functional monomer system with the expectation that, upon rebinding of the atrazine molecule, the fabricated MIPP could change its hydrogel volume sufficiently to cause the color change in the whole visible-light wavelength range. Considering the increase in the hydrophilic nature and reduced stereo-hindrance effect, acrylic acid (AA) was chosen as the functional monomer to prepare new MIPP films with improved sensing properties towards atrazine.

Sensing properties of AA-based MIPP films: By using the same preparation procedure, an AA-based MIPP film was first fabricated by using the pre-polymerization mixture with an atrazine/AA/EGDMA ratio of 1:4:1.5. Figure 3 displays the sensing behavior of the resulting MIPP film with a series of concentrations of atrazine. Indeed, we found that the AA-based MIPP films show a higher sensitivity at the same atrazine concentration than the MAA-based MIPP films (Figure 3A,B). Atrazine at a concentration of 10^{-12} M already induced a Bragg diffraction shift of 13 nm. At 10^{-6} M atrazine, a remarkable shift of over 170 nm from 448 nm to 620 nm was achieved. More importantly, in a broad concentration range from 10^{-12} M to 10^{-6} M, the sensing of atrazine by using AA-based MIPP is accompanied by distinct color changes, which almost cover the whole visible-light wavelength range from blue light to red light, and can therefore be discriminated by the naked eye (Figure 3C).

Compared with MAA-based MIPP, it should be noted that the intensity of the optical diffraction of AA-based MIPP decreased monotonically as the atrazine rebinding process progressed (Figure 3A,B). After the film had been soaked in 10^{-9} M atrazine solution, the intensity of the diffraction peak dropped to half of that of the original MIPP film. As the concentration of atrazine was increased to 10^{-6} M, a broad and weak diffraction peak was observed. A similar phenomenon was also noticed by other groups.[16] The inverse relationship between the diffraction peak intensity and the diffraction shifts of the hydrogel can be induced by different factors, including a decrease in the refractive index contrast during film swelling, an increasing presence of disorder in the swollen hydrogel, or partial pore closure during hydrogel expansion.[16] In our case, we believe that the increased disorder of the swollen hydrogel upon the rebinding of atrazine is a possible reason for this phenomenon. Nevertheless, this diffraction response is reversible and the disorder of the swollen gel is temporal. When the film is soaked in acetic acid solution, the well-defined diffraction peak can be recovered.

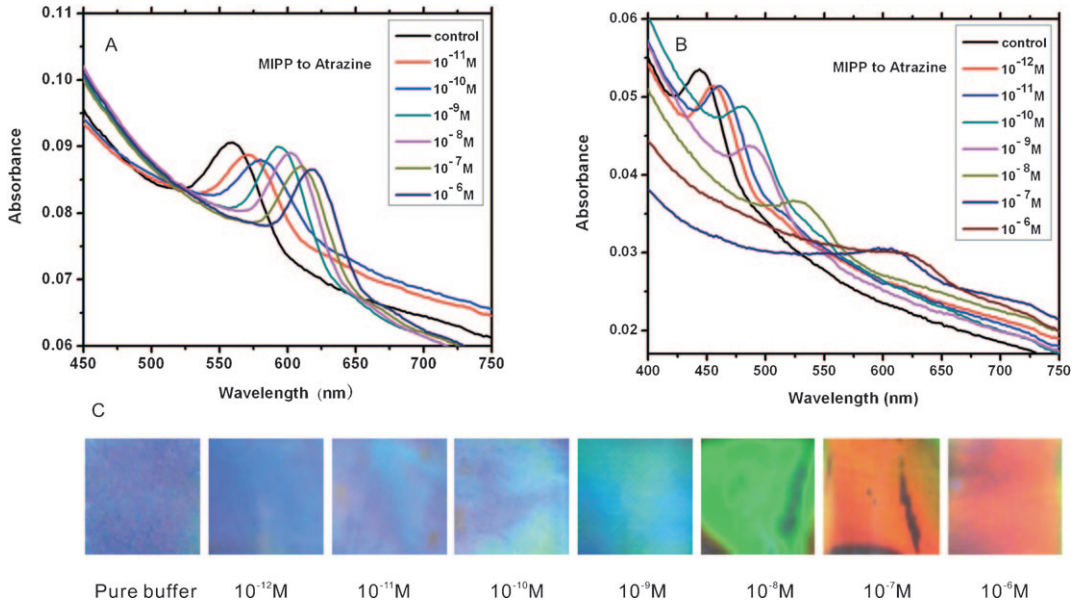

Figure 3. Optical response of MIPP films fabricated by using different functional monomers to atrazine with various concentration: A) MAA as the functional monomer; B) AA as the functional monomer; C) color change induced by the rebinding of atrazine at different concentrations (shown for the case of the MIPP film fabricated by using AA as the functional monomer).

For the efficient detection or sensing of the targeted molecule, ideally, the resulting hydrogel film should have the following structure and properties: a) a 3D-ordered and interconnected macroporous structure should be formed by colloidal-crystal templating to produce a well-defined optical signal (Bragg diffraction) and allow the favorable diffusion of the detected molecule inside the hydrogel film; b) the nanocavities resulting from molecular imprinting should exhibit high affinity and specificity and be easily accessible to the hydrogel film; and c) the molecular recognition events within the nanocavities should induce obvious swelling or shrinkage of the hydrogel film with a readable optical signal. These desirable structures and properties described above are closely related to the selectivity, sensitivity, and responsiveness of the prepared film for sensing atrazine. In fact, we found that these structure and related properties are somewhat contradictory. For example, to maintain the integrity of the 3D-ordered macroporous structure and to obtain nanocavities with high specificity, more cross-linking is required to form rigid frameworks, which inevitably leads to difficulties associated with the release and uptake of atrazine molecules and inhibits the formation of highly flexible polymers for swelling or shrinkage. Hence, the optimization of the hierarchically structured hydrogel film and associated properties become quite complex. To achieve the optimal conditions or 'recipe' for constructing the desired sensors in this work, the molar ratio between the functional monomer (AA) and cross-linker (EGDMA) as the key influence factor was investigated.

Figure 4 presents the atrazine-dependent optical response of the MIPP films that were prepared by using the following molar ratios: a) AA/EGDMA = 4:1; b) AA/EGDMA = 4:1.5, and c) AA/EGDMA = 4:2. As expected, with the increased use of the cross-linker, less diffraction peak shift was observed and the capacity of the resulting EIPP response to atrazine recognition decreased. When the molar ratio of AA to EGDMA is 4:2, the EIPP hydrogel exhibits an overall 30-nm shift (Figure 4C), whereas the overall shift is increased to 68 nm in the case of the EIPP using a molar ratio of 4:1.5 (Figure 4B). In contrast, when we decreased the molar ratio to 4:1, the peaks shifted by more than 170 nm (Figure 4A). For a better comparison, wavelength shifts versus atrazine concentration was plotted instead of raw data (Figure 4D). With a further decrease in the molar ratio (for example 4:0.5), however, we found that the amount of the cross-linker used was not enough to maintain the 3D-ordered porous framework, and as a result the Bragg diffraction peak disappeared, leading to an ill-defined optical signal (not shown). As discussed above, the reason for these results is not hard to understand. To balance the

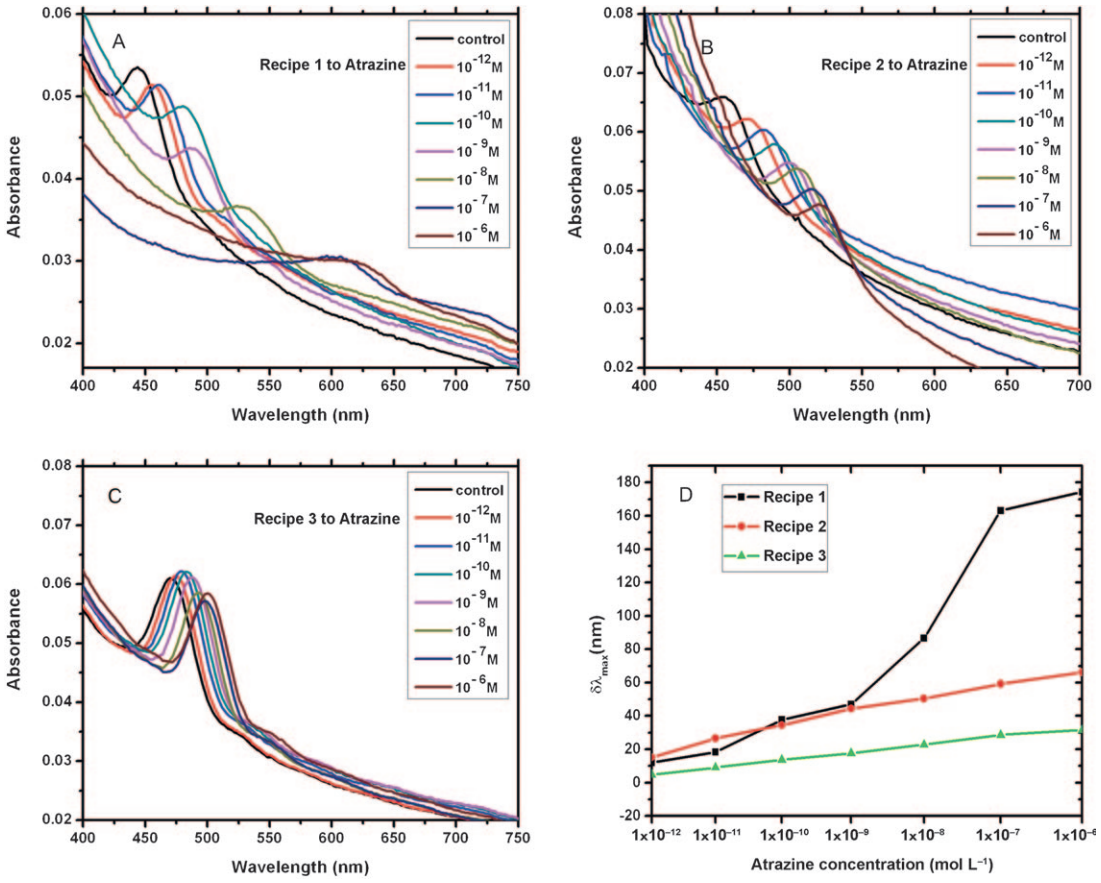

Figure 4. Optical response of AA-based MIPP films fabricated by using different polymerization recipes for atrazine at various concentrations: A) AA/EGDMA = 4:1; B) AA/EGDMA = 4:1.5; C) AA/EGDMA = 5:2; D) plots of Bragg shifts of AA-based MIPP films versus atrazine concentrations.

above-mentioned contradiction, the molar ratio of 4:1 (AA/EDGMA) was fixed for the fabrication of our MIPP film and used in the following experiments.

Selectivity of AA-based MIPP film: The selectivity test of an atrazine-imprinted photonic polymer prepared from AA and EGDMA was carried out by using two 1,3,5-triazines (ametryn and prometryn), which are structurally similar to atrazine, as well as one structurally unrelated herbicide (2,4-dichlorophenoxyacetic acid, 2,4-D) as the reference compounds (see Scheme 1). The optical responses of the MIPP film to these reference herbicides are shown in Figure 5.

Compared with the results in Figure 4A, it is seen that ametryn or prometryn, which display only very small structural differences to atrazine (Scheme 1), can only induce slight optical shifts under the same measurement conditions (Figure 5A, B). Although the recognition is not absolutely specific to atrazine, this result clearly indicates that such an MIPP film is able to efficiently discriminate between triazine herbicides. The selectivity of atrazine-imprinted polymers has also been investigated by several groups previously, and similar results were also observed. For example, Kubo and co-workers studied the selectivity of atrazine-imprinted polymers and found that other triazines could also bind to the imprinted polymer by 10–30% when compared with atrazine.[7] The reason is believed to be that the structure and hydrogen-bonding sites of triazine are very similar to those of atrazine. Remarkably, however, the structurally unrelated herbicide 2,4-D did not cause any perceptible optical response of the MIPP film at all (Figure 5C). These results suggest that the selectivity of the MIPP film for atrazine was clearly induced during the molecular imprinting process. Owing to the complementary shape, size, and interaction sites with the formed binding sites, only atrazine rather than other herbicide molecules can specifically occupy the imprinted nanocavities within the MIPP film and cause the volume change of the hydrogel film, thereby inducing the shift of the Bragg diffraction peak. The fact that the prepared MIPP can delicately discriminate between the very similar triazine molecules and other herbicides suggests that the cooperative effect of shape, size, and interaction sites of the formed biding sites plays a critical role in the high-selectivity molecular recognition process of MIPP. As a comparison, Figure 5D shows the high specificity of the prepared MIPP film for atrazine against other herbicides. To further elucidate the molecular recognition properties of the imprinted materials, the nonimprinted 3D-ordered macroporous hydrogels (NIPP) as a control sample were also synthesized under the same preparation conditions as the imprinted photonic polymer, but in the absence of atrazine tem-

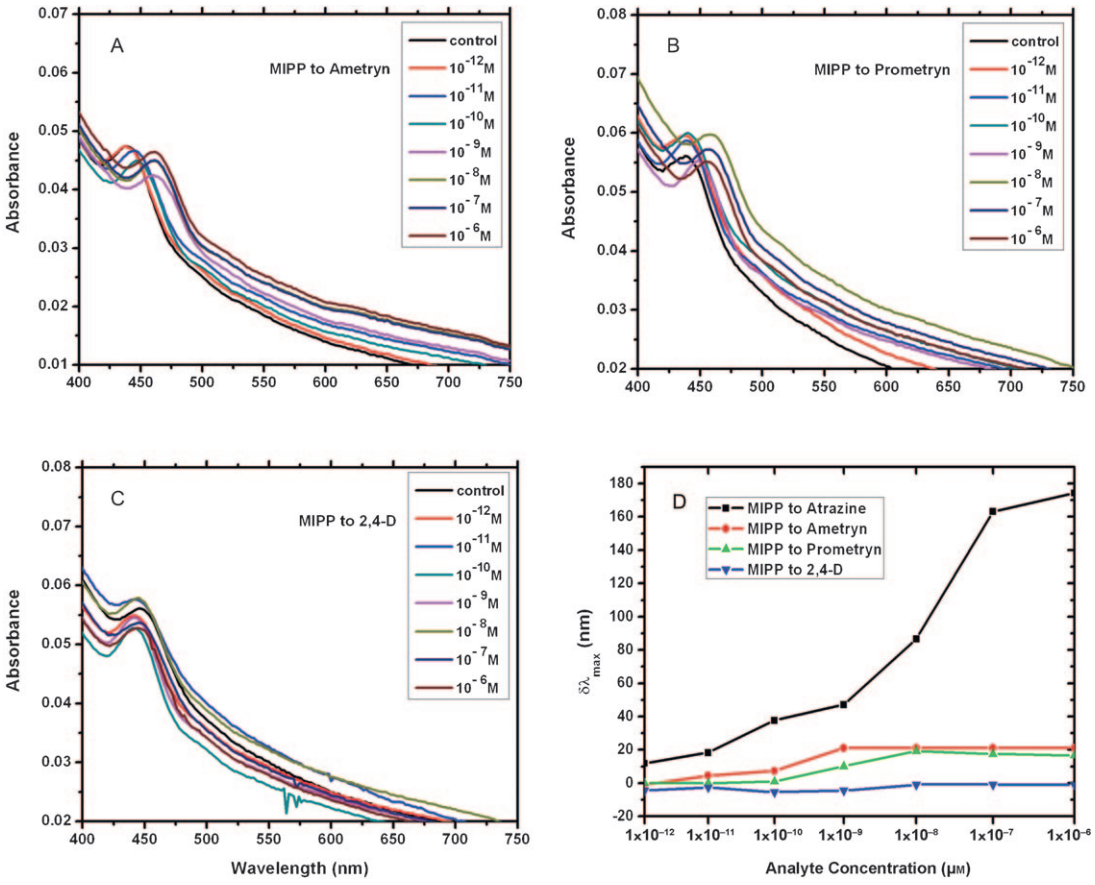

Figure 5. Optical response of the atrazine-imprinted photonic polymer to other herbicides: A) ametryn; B) prometryn; C) 2,4-D; D) plots of Bragg shifts of MIPP to different herbicides with various concentrations.

plates. Figure 6 displays the evolution of the diffraction peak of the nonimprinted photonic film (NIPP) upon exposure to a phosphate buffer solution containing atrazine or reference herbicides as a function of concentration. Probably owing to some nonspecific adsorption, only a slight fluctuation in the Bragg peak was observed in the case of the nonimprinted hydrogel film, which is quite different from the recognition behavior exhibited by the prepared MIPP (Figure 4). These results described above clearly indicate that the microenvironments created by molecular imprinting are responsible for the observed results of atrazine-imprinted photonic polymers.

Rapid response and recoverability of AA-based MIPP films: Besides producing a readable optical signal, the 3D-ordered interconnected macroporous structure is characterized by a high surface-to-volume ratio. This structural feature cannot only provide more complete removal of imprinted molecules to achieve a high density of efficient recognition sites. More importantly, this structure is favorable for molecular diffusion and most of the created recognition sites are situated at the surface or in proximity to the surfaces of the ultrathin polymer wall, which provides a better site accessibility and lower mass-transfer resistance. Indeed, we found that the prepared MIPP film exhibits a very fast response time, and the atrazine rebinding process can be completed within 30 s (Figure 7A). Generally, the established methods for determining atrazine need considerable time. For chromatographic methods, it usually takes tens of minutes to separate the analyte before determination.[28] For immunochromatography methods,[1,3] it will take several minutes to get a result. An electrochemically based atrazine sensor's response time is usually in the order of 30 min.[5–6]

As the MIPP films are of a highly cross-linked polymeric nature, the MIPP films also show good physical stability and chemical inertness. These IPP films can be easily recovered by elution by using acetic acid/methanol to remove rebinding analytes followed by rinsing with a neutral phosphate buffer solution to restore the neutral blank status. Figure 7B shows the recoverability of a MIPP film over five cycles. The standard error is within 5%, which is indicative of good reproducibility.

Adsorption capacities of AA-based MIPP films in water: To gain insight into the binding performance of the atrazine-imprinted photonic polymer, adsorption experiments and subsequent Scatchard analysis were carried out. In Figure 8, the amount (Q) of atrazine bound to MIPP or NIPP was plotted against various initial concentrations of atrazine. From the isotherm curves, it is clear that the adsorption of MIPP in-

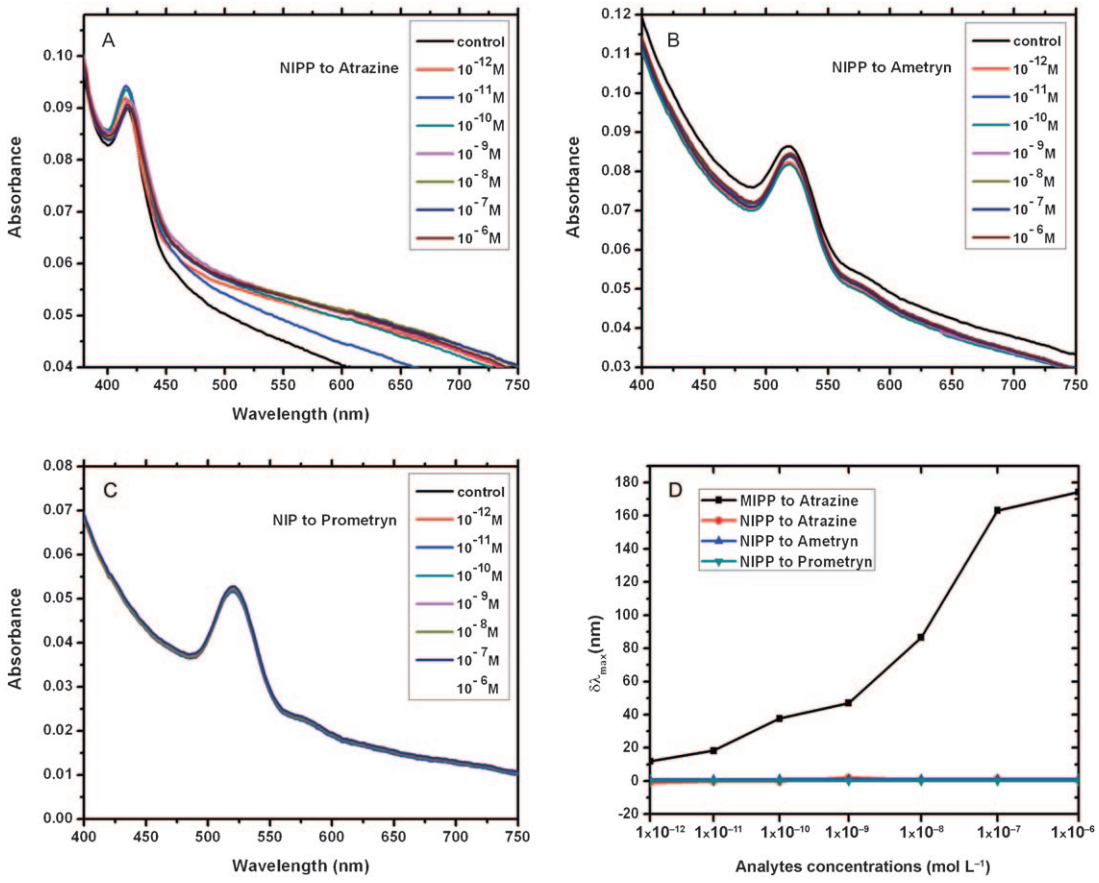

Figure 6. Optical response of non-imprinted photonic polymer (NIPP) to different herbicides: A) ametryn; B) atrazine; C) prometryn; D) plots of the Bragg shift of NIPP with different herbicides at various concentrations.

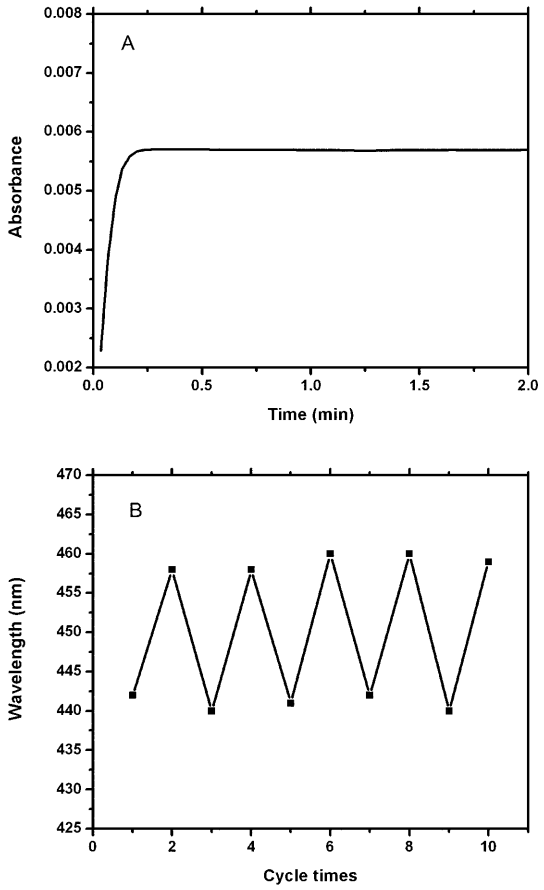

Figure 7. Kinetic response (A) and recoverability (B) of AA-based MIPP Film.

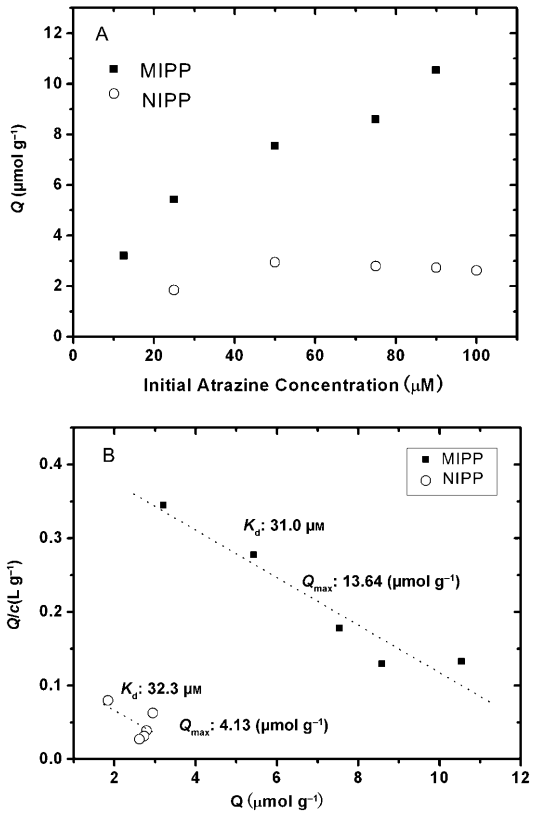

Figure 8. Binding isotherm (A) and Scatchard plot (B) of the atrazine-imprinted photonic polymer (MIPP) and non-imprinted photonic film (NIPP).

creased greatly with the increased atrazine concentrations, whereas the adsorption of NIPP only increased slightly with the concentrations. This result suggests that the imprinted polymer MIPP is a better binder for atrazine, possibly owing to the presence of a large number of binding sites within the polymer network. We also found that the imprinted polymer is not saturated and there is a tendency to adsorb more atrazine molecules if the concentration is higher. However, since the solubility of atrazine in the water does not exceed 33 mg L^{-1} (about 100 μM); the maximum concentration of 100 μM was used in the adsorption experiments. The obtained binding data were analyzed to estimate the dissociation constant (K_d) and the number of binding sites (Q_{max}). We also performed several investigations involving the estimation of the binding affinity of atrazine-imprinted polymer in organic solvents. It was found that the Scatchard plot was not linear, suggesting that the binding sites are heterogeneous with respect to the affinity for atrazine.[27–28] In our experiment, however, we obtained only one line with a K_d value of 31.0 μM and $Q_{max} = 13.64$ μmol g^{-1} for the MIPP film. One reason for these differences may lie in the different concentration range, as the concentration of atrazine in organic solvents can be as high as several mM. At high concentration values, another adsorption line could also be observed. Also, a different solvent medium has considerable influence on the adsorption behavior of polymers. Some of our experiments revealed that water could disturb the formation of hydrogen bonding and disturbed the adsorption property of the molecular imprinted polymers. Water has a high polarity and is unfavorable for the formation of hydrogen bonds. However, all our experiments were carried out in aqueous solutions and our MIPP showed selective and adsorptive properties. This suggests that in our inverse opal hydrogel polymer (MIPP), the formation of hydrogen bonds actually occurred and that a considerable number of rebinding sites are formed. Compared with MIPP, the linearity of the measured data is very poor in the case of NIPP (Figure 8B). It is roughly estimated that NIPP has 4.13 μmol g^{-1} (Q_{max}) and 32.3 μM (K_d). Obviously, MIPP has a larger adsorption capacity than NIPP. However, in our case, it is difficult to understand why NIPP displays similar dissociation constants to MIPP. This result seems to be contradictory to the high selectivity of MIPP that is described above. Accordingly, we are now studying this aspect in detail to find an explanation for this phenomenon.

From Figure 8, it can be seen that the mass content of the analyte in the MIP in the optical studies is well below 0.1% at the low concentrations that were used. The swelling of the inverse opal lattice should thus be the dominating effect. The low atrazine concentration can induce dramatic swelling

of the prepared inverse opal. The probable reason for this observation is the buildup of a Donnan potential between the polymer hydrogel phase and the bulk solution phase during the rebinding process of atrazine molecules to MIP. As the atrazine molecule is also a base, the rebinding process could also cause the increase in the degree of ionization on the MIP through an acid–base reaction between atrazine and carboxy groups of MIP. As a result, a Donnan potential is builds up between the two phases and the resulting influx of solvent and ions leads to polymer hydrogel swelling, which may be detected as a redshift in optical diffraction. A similar phenomenon was also observed previously.[16] Nevertheless, the dramatic swelling is very remarkable. Compared to other hydrogels with partly ionic groups, the change in density with charge is never as large. Further work to explain these differences is underway.

Conclusion

We have developed a new strategy for the convenient and ultrasensitive detection of atrazine based on photonic-crystal and molecular imprinting techniques. The constructed sensory system is characterized by a) simultaneously possessing high sensitivity and specificity, quick response, and good regenerating ability in an aqueous environment; b) directly generating readable optical signals (colorimetric) suitable for reporting recognition events without any necessary treatments for analytes (label-free) or the use of complex instruments. The general applicability of this new approach and the distinguished features indicate that MIPPs could also be used in arrays of optical sensors in which each individual sensor will detect different herbicides. It is envisaged that the formed arrays could function as a "pH"-like paper and provide a promising alternative for rapid monitoring of atrazine levels on the spot.

In the few last years, the development of MIPs has been impressive in both breadth of template and also diversity.[33] However, as one of the most important application areas of the molecular imprinting technique, the construction of MIP-based sensors requires the integration of additional transduction elements. Thus, how to develop "smart MIP" that can directly transfer the molecular recognition process into a readable signal is highly desirable in this area.[34] The concept reported herein provides a new means to construct such "smart MIPs". We believe that such a concept could not only have an important impact on the development of MIP-based sensory applications, but also extend the application scope of photonic materials.

Experimental Section

Materials and chemicals: Atrazine, ametryn, prometryn, 2,4-dichlorophenoxyacetic acid (2,4-D), methacrylic acid (MAA), acrylic acid (AA), and tetraethoxysilane (TEOS) were purchased from Beijing Chemical Industries. Ethylene glycol dimethylacrylate (EGDMA) and 2,2′-azobisisobutyronitrile (AIBN) were obtained from Arcos Organics. Anhydrous ethanol, ammonia, acetic acid, glycol, and other affiliated chemicals were all from local suppliers. All solvents and chemicals are of reagent quality and were used without further purification. Common glass slides were cut to be $50\times20\,mm^2$ and immersed in a H_2SO_4/H_2O_2 mixture for 12 h, followed by rinsing with deionized water in an ultrasonic bath three times and then dried prior to use. All 7-mL vials for the formation of colloidal-crystal templates were cleaned by rinsing with the H_2SO_4/H_2O_2 mixture and deionized water. Polymethyl methacrylate (PMMA) slides (50 mm long, 20 mm wide and 1.5 mm thick) as supports for the formed EIPP film were cleaned with anhydrous ethanol. NaH_2PO_4 and Na_2HPO_4 were used as buffer solution at pH 7.6 for all molecular sensing measurements.

Formation of colloidal-crystal templates: The highly uniform silica colloidal microspheres were synthesized by using an approach based on the Stöber method.[23] In a typical preparation, TEOS (8.74 g) and anhydrous ethanol (180 mL) were mixed in a 250-mL flask and stirred with a magnetic beater. Then, ammonia (15.4 mL) and deionized water (4.46 g) were slowly added and the resulting reaction mixture was left overnight. After centrifugation and dispersion with anhydrous ethanol had been repeated four or five times to expunge residues, the monodispersed silica particles were obtained and fully dispersed in anhydrous ethanol (weight concentration ca. 1–4%), which were allotted into 7-mL clean vials for the formation of colloidal-crystal templates. A clean glass slide was vertically placed into each vial for colloidal-crystal growth.[24] After complete volatilization of ethanol, silica colloidal-crystal templates were formed on both sides of each glass slide.

Synthesis of molecularly imprinted photonic polymers (MIPP): To achieve multipoint interacting binding sites of high selectivity in the resulting photonic polymer, excess functional monomer was added. In our work, we fixed the molar ratios between atrazine and MAA or AA at 1:4. In a typical preparation for MIPP, atrazine (1 mmol, 216 mg), MAA (4 mmol, 344 mg) and EGDMA (1 mmol, 0.2 mL) were mixed overnight in methanol (0.5 mL) to allow sufficient complexation. Then, AIBN (6.1 mmol, 0.01 g) was added, and the mixture was degassed with nitrogen for 10 min. Glass slides with a colloidal-crystal film were coated with a PMMA slide and held together to retain the above-mentioned precursor mixture. Once the colloidal crystal of the formed sandwich structure became transparent, a successful infiltration process was completed. After the removal of excess precursors, photopolymerization was performed in an ice bath under a UV light at 365 nm for 2 h. The sandwiches were immersed in 1% hydrofluoric acid for 2 h to separate the double slides and fully etch the used silica particles. The formed polymer films remained on the PMMA substrate. The embedded atrazine molecules were removed by incubating the polymer film in an acetic acid/methanol mixture for 6 h, followed by rinsing with phosphate buffer solution (pH 7.6). For control experiments, non-imprinted photonic hydrogel (NIPP) films were also prepared by using the same procedure and conditions, only without the addition of atrazine molecules.

Characterization: UV/Vis spectra were carried out on a UV/Vis spectrometer (PerkinElmer Lambda35). Surface morphologies of the used templates and the resultant EIPP films were observed by using a KYKY 2800 scanning electron microscope operating at 25 kV. The photopolymerization was implemented under UV light (FUSI Electric ST3; 16 W). A centrifuging apparatus (Anke TDL-60B, Shanghai, China) was used for the centrifugation of colloidal particles from the reactants. The sensing properties of the fabricated MIPP were checked by exposure to solutions of the analyte (atrazine, ametryn, and prometryn) one after another from low to high concentrations in buffer solution. The shift of the Bragg diffraction wavelength of EIPP after the exposure was measured by using a UV/Vis spectrometer. The color change of the EIPP films were obtained by using a common digital camera under a daylight lamp.

Scathchard analysis:[25] The free-standing molecularly imprinted or non-imprinted photonic polymers were dried in the oven after the removal of both templates (silica particles and atrazine molecules). Typically, the polymer (10 mg) was immersed in an aqueous solution of atrazine (10 mL) at various concentrations ranging from 5–100μM at room temperature. After incubation for 6 h, the sample was centrifuged, and the upper clear

solution was subjected to concentration analysis of the remaining atrazine. Q/C_{eq} is plotted versus C_{eq} according to the equation, $Q/C_{eq} = (Q_{max} - Q)/K_d$, where Q is the amount of bound atrazine ($\mu mol\,g^{-1}$), C_{eq} the concentration of the free atrazine (mM), Q_{max} the apparent maximum number of binding sites ($\mu mol\,g^{-1}$), and K_d the equilibrium dissociation constant.

Acknowledgement

We gratefully acknowledge the financial support from the National Science Foundation of China (20473044, 20533050, and 50673048), 973 Program (2006CB806200), and the transregional project (TRR6).

[1] W. B. Shim, Z. Y. Yang, J. Y. Kim, J. G. Choi, J. H. Je, S. J. Kang, A. Y. Kolosova, S. A. Eremin, D. H. Chung, *J. Agric. Food Chem.* **2006**, *54*, 9728.
[2] N. Graziano, M. J. Mcguire, A. Roberson, C. Adams, H. Jiang, N. Blute, *Environ. Sci. Technol.* **2006**, *40*, 1163.
[3] J. Kaur, K. V. Singh, R. Boro, K. R. Thampi, M. Raje, G. C. Varshney, R. C. Suri, *Environ. Sci. Technol.* **2007**, *41*, 5028.
[4] S. B. Huang, T. J. Mayer, R. A. Yokley, R. Perez, *J. Agric. Food Chem.* **2006**, *54*, 713.
[5] S. A. Piletsky, E. V. Piletskaya, A. V. Elgersma, K. Yano, I. Karube, *Biosens. Bioelectron.*, **1995**, *10*, 959.
[6] T. Panasyuk-Delaney, V. M. Mirsky, M. Ulbricht, O. S. Wolfbeis, *Anal. Chim. Acta*, **2001**, *435*, 157.
[7] R. Shoji, T. Takeuchi, I. Kubo, *Anal. Chem.* **2003**, *75*, 4882.
[8] A. Stein, F. Li, N. R. Denny, *Chem. Mater.* **2008**, *20*, 649.
[9] Y. J. Lee, C. E. Heitzman, W. R. Frei, H. T. Johnson, P. V. Braun, *J. Phys. Chem. A* **2006**, *110*, 19300.
[10] R. A. Barry, P. Wiltzius, *Langmuir* **2006**, *22*, 1369.
[11] H. Saito, Y. Takeoka, M. Watanabe, *Chem. Commun.* **2003**, *2126*.
[12] Y. Takeoka, M. Watanabe, *Adv. Mater.* **2003**, *15*, 199.
[13] D. Nakayama, Y. Takeoka, M. Watanabe, K. Kataoka, *Angew. Chem.* **2003**, *115*, 4329; *Angew. Chem. Int. Ed.* **2003**, *42*, 4197.
[14] K. Matsubara, M. Watanabe, Y. Takeoka, *Angew. Chem.* **2007**, *119*, 1718; *Angew. Chem. Int. Ed.* **2007**, *46*, 1688.
[15] Y. J. Lee, P. V. Braun, *Adv. Mater.* **2003**, *15*, 563.
[16] Y. J. Lee, S. A. Pruzinsky, P. V. Braun, *Langmuir* **2004**, *20*. 3096.
[17] X. Hu, Q. An, G. Li, S. Tao, J. Liu, *Angew. Chem.* **2006**, *118*, 8325; *Angew. Chem. Int. Ed.* **2006**, *45*, 8145.
[18] K. Haupt, K. Mosbach, *Chem. Rev.* **2000**, *100*, 2495.
[19] G. Wulff, *Chem. Rev.* **2002**, *102*, 1.
[20] L. Ye, K. Mosbach, *Chem. Mater.* **2008**, *20*, 859.
[21] *Molecular Imprinting-From Fundamentals to Applications* (Eds.: M. Komiyama, T. Takeuchi, T. Mukawa, H. Asanuma), Wiley-VCH, Weinheim, Germany, **2002**.
[22] *Molecularly Imprinted Polymers: Man-Made Mimics of Antibodies and Their Application in Analytical Chemistry* (Ed.: B. Sellergren), Elsevier, Amsterdam, **2001**.
[23] W. Stoeber, A. Fink, E. Bohn, *J. Colloid Interface Sci.* **1968**, *26*, 62.
[24] P. Jiang, K. S. Hwang, D. M. Mittleman, J. F. Bertone, V. L. Colvin, *J. Am. Chem. Soc.* **1999**, *121*, 11630.
[25] M. Quaglia, K. Chenon, A. J. Hall, E. De Lorenzi, B. Sellergren, *J. Am. Chem. Soc.* **2001**, *123*, 2146.
[26] B. Dirion, Z. Cobb, E. Schillinger, L. I. Andersson, B. Sellergren, *J. Am. Chem. Soc.* **2003**, *125*, 1501.
[27] J. Matsui, S. Goji, T. Murashima, D. Miyoshi, S. Komai, A. Shigeyasu, T. Kushida, T. Miyazywa, T. Yamada, K. Tamaki, N. Sugimoto, *Anal. Chem.* **2007**, *79*, 1749.
[28] J. Matsui, K. Fujiwara, T. Takeuchi, *Anal. Chem.* **2000**, *72*, 1810.
[29] J. Matsui, Y. Miyoshi, O. Doblhoff-Dier, T. Takeuchi, *Anal. Chem.* **1995**, *67*, 4404.
[30] M. Siemann, L. I. Andersson, K. Mosbach, *J. Agric. Food Chem.* **1996**, *44*, 141.
[31] F. Chapuis, V. Pichon, F. Lanza, B. Sellergren, M.-C. Hennion, *J. Chromatogr. B* **2004**, *804*, 93.
[32] M. T. Muldoon, L. H. Stanker, *Anal. Chem.* **1997**, *69*, 803.
[33] C. Alexander, H. S. Andersson, L. I. Andersson, R. J. Ansell, N. Kirsch, I. A. Nicholls, J. O'Mahony, M. J. Whitecombe, *J. Mol. Recognit.* **2006**, *19*, 106.
[34] A. McCluskey, C. I. Holdsworth, M. C. Bowyer, *Org. Biomol. Chem.* **2007**, *5*, 3233.

Received: June 24, 2008
Revised: September 24, 2008
Published online: November 14, 2008

